Orogen-parallel mass transport along the arcuate Himalayan front into Nanga Parbat and the western Himalayan syntaxis

David M. Whipp (david.whipp@helsinki.fi)
Department of Geosciences and Geography
University of Helsinki, Finland

Christopher Beaumont
Department of Oceanography
Dalhousie University, Canada

X2.105

1. Introduction

The rates of Quaternary rock uplift in the Nanga Parbat region of the western Himalayan syntaxis are 2-3 times those observed in the central Himalaya. This difference suggests the crustal mass flux into the Nanga Parbat region must be significantly higher than in the central Himalaya to sustain the high topography. One possible mechanism for supplying this mass is strain partitioning across the arcuate thrust front, which produces an orogen-parallel mass flux along strike into the Nanga Parbat region where the convergence obliquity angle rapidly decreases and orogen-parallel crustal shortening will occur.

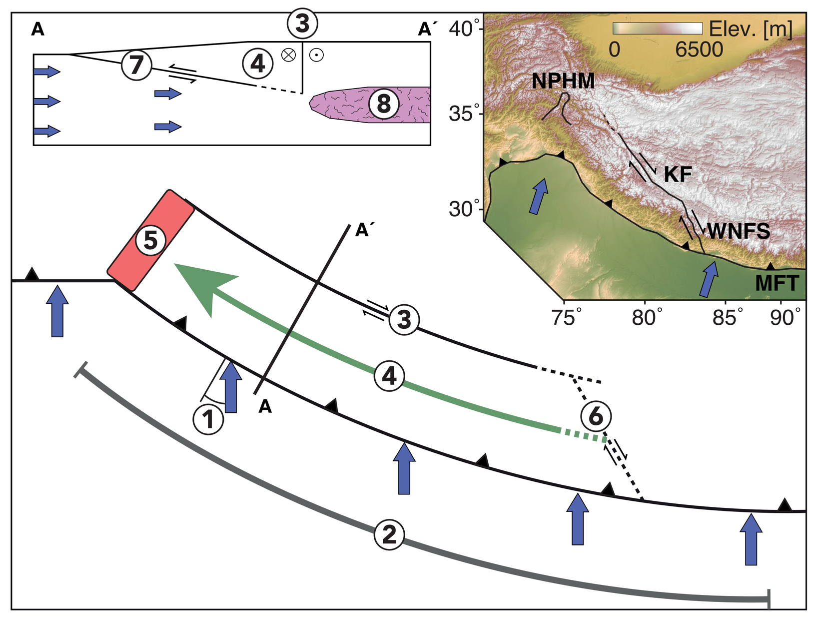

Figure 1. Schematic diagram of the geodynamic components of an arcuate orogen. Map view of main components (listed below). Left inset: Cross-section A-A´in the central part of the arc where strain is partitioned. Right inset: Topographic map of the Himalaya and Tibet with major tectonic structures and convergence vectors (blue). NPHM: Nanga Parbat-Haramosh Massif; KF: Karakoram fault; WNFS: Western Nepal Fault System (Murphy et al., 2014); MFT: Main frontal thrust

Components of a strain-partitioned arcuate convergent orogen (see labels above)

① Obliquity between the thrust front and the convergence velocity vector
② Arcuate thrust front with increasing obliquity along strike
③ Strike-slip structure at rear of orogenic wedge
④ Orogen-parallel mass flux owing to strain partitioning at the thrust front
⑤ Shortening at end of oblique zone where the obliquity rapidly decreases
⑥ Strike-slip/extensional structure accommodating transition from oblique thrusting to partitioned strain
⑦ Low inclination detachment below critical wedge
⑧ Weak, viscous middle-lower crust beneath an orogenic plateau

Problems addressed in this study:
- How is strain partitioned along strike in arcuate orogens?
- How does strain partitioning in arcuate orogens affect mass transfer along strike?

2. Strain partitioning theory

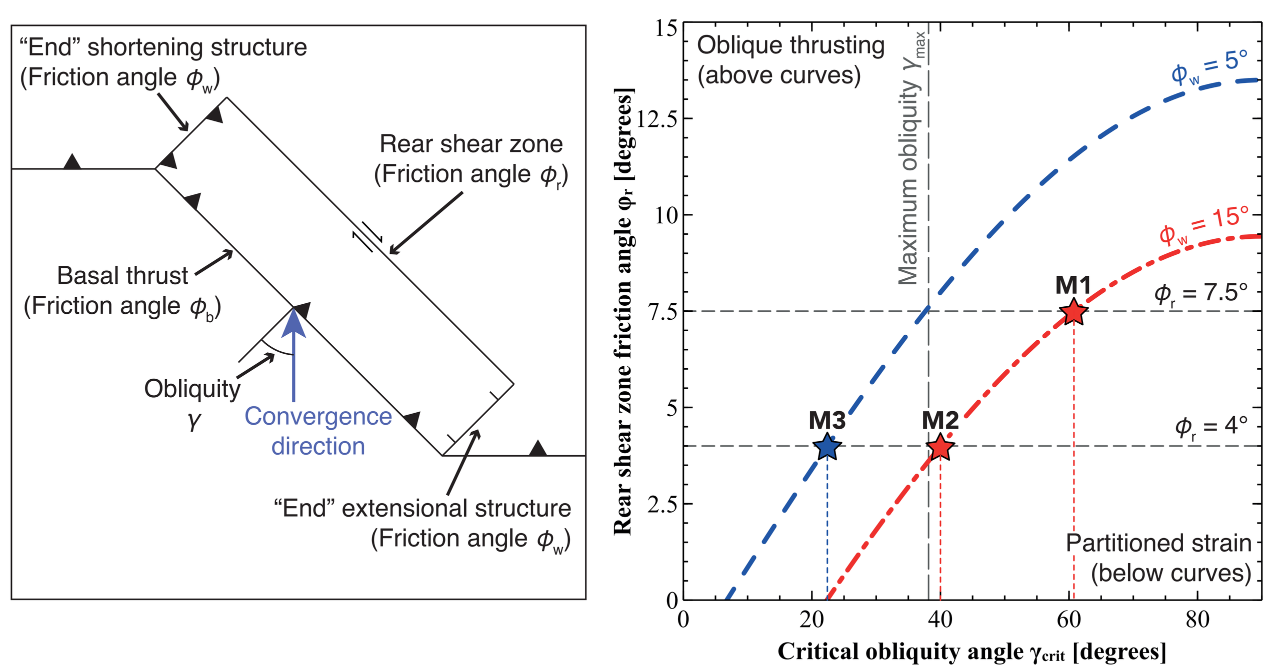

Figure 2. Predictions for strain partitioning behavior from a 3D force balance in a segmented linear orogen. (Left) Generalized geometry of a 3D orogen with an obliquely convergent linear segment bounded by segments of normal convergence. (Right) Predictions for conditions under which strain partitioning will occur for a segmented linear orogen of the scale of the Himalaya. Strain partitioning will occur at decreasing convergence obliquity angles γ_{crit} as the strength of the rear shear zone decreases. Furthermore, decreasing the strength of the orogenic wedge from 15° (red) to 5° (blue) also favors partitioning at smaller values of γ_{crit}. M1, M2, and M3 indicate the material properties used in Models 1-3 (see Results).

Whipp et al. (2014) presents an analytical relationship for predicting the conditions under which strain partitioning will occur in a segmented linear orogen based on a balance of the forces acting on the base, rear, and either end of the orogenic wedge (Figure 2). Using this force balance model for the scale of the Himalaya, we can *estimate* the conditions under which strain partitioning will occur for the arcuate orogen assuming strain partitioning will only develop where the convergence obliquity exceeds the critical obliquity angle γ_{crit}. The maximum obliquity angle in the Himalaya is ~38° (Figure 2, right).

Thus, we predict no strain partitioning for a relatively strong rear shear zone with ϕ_r = 7.5° (point M1), strain partitioning of only the most oblique part of the arc for a weak rear shear zone with ϕ_r = 4° and strong wedge with ϕ_w = 15° (point M2), and strain partitioning in about half the arc for a weak rear shear zone with ϕ_r = 4° and weak wedge with ϕ_w = 5° (point M3).

3. Model design

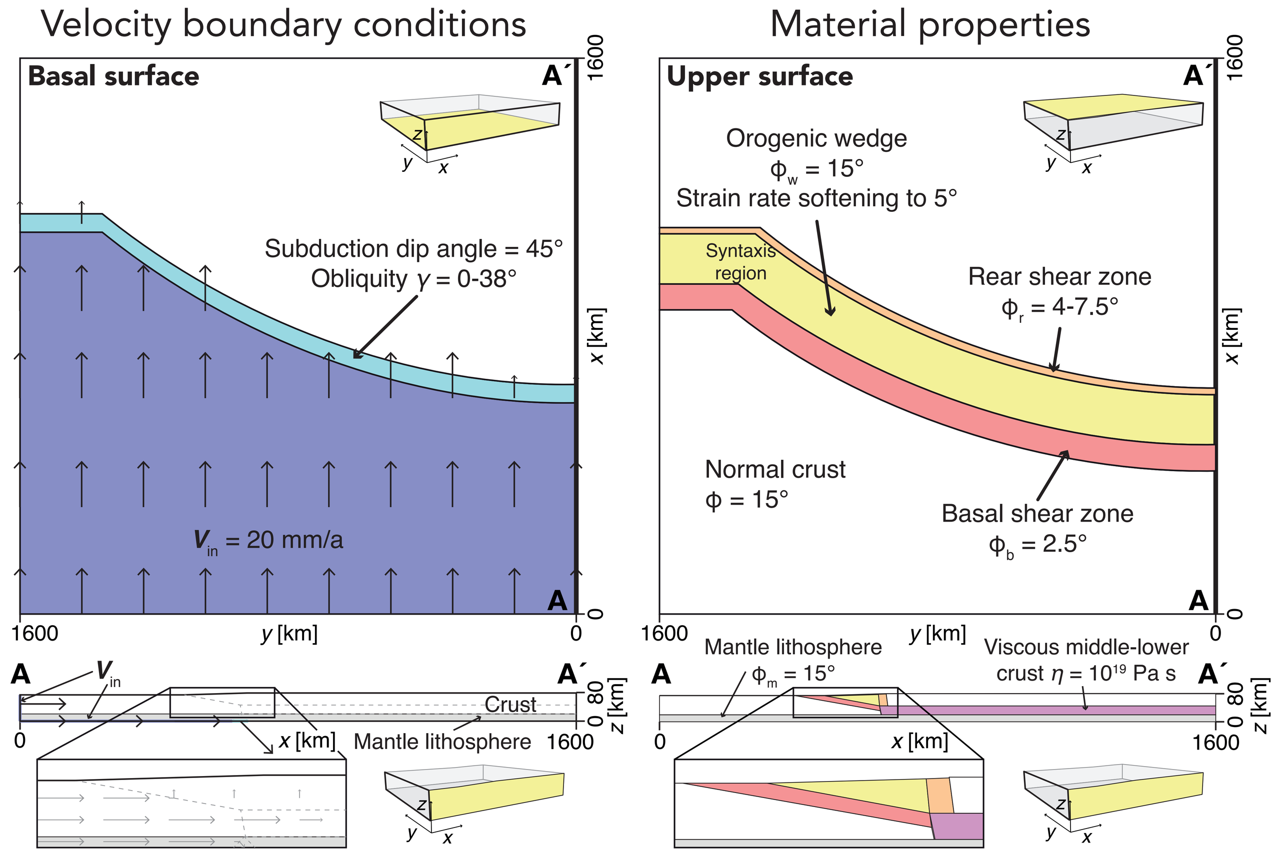

Figure 3. Numerical experiment velocity boundary conditions and material properties. (Left) Oblique collision results from a flux of mass into the side of the model at x=0 (medium blue) and subduction of the mantle lithosphere along an arcuate region with an obliquity up to 38° (light blue). (Right) Model mechanical properties are defined in arcuate zones corresponding to the basal shear zone (pink), orogenic wedge (yellow), rear shear zone (orange), viscous middle-lower crust (purple), normal crust (white), and mantle lithosphere (gray).

Numerical experiments here use the 3D finite-element creeping flow software DOUAR (Braun et al., 2008) to simulate oblique continental collision and mantle lithosphere subduction driven by prescribed velocity boundary conditions. The models are purely mechanical, with either Mohr-Coulomb frictional plasticity or linear viscosity. The general geometry is based on a mature orogen with an orogenic wedge adjacent to an orogenic plateau. Additional model parameters are below.

Parameter	Value
Spatial scale	1600 x 1600 x 80 km
Element size	6.25 x 6.25 x 3.125 km
Time step	50,000 a
Plateau height	5 km
Orogenic wedge surface slope	1.79°
Crustal density	2750 kg m^{-3}
Mantle density	3300 kg m^{-3}
Cohesion (all frictional materials)	1 MPa

4. Results

Model 1 - Strong rear shear zone (ϕ_r = 7.5°): No strain partitioning

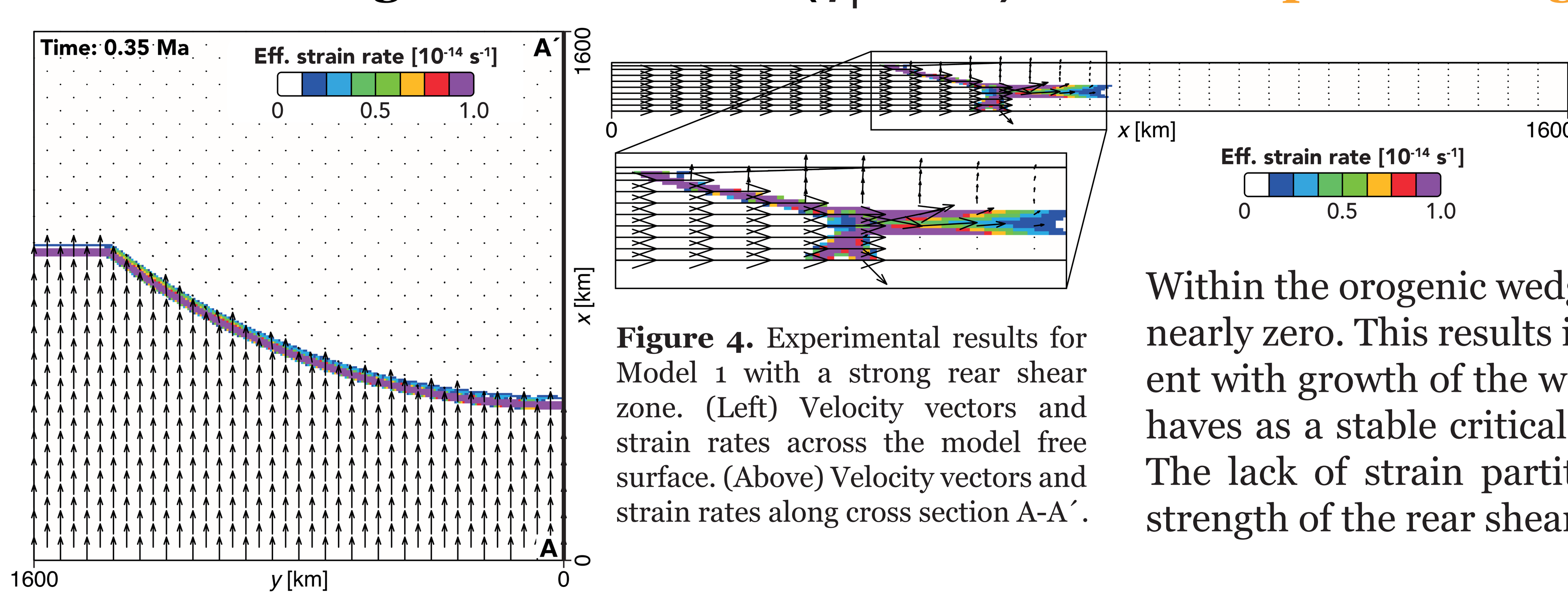

Figure 4. Experimental results for Model 1 with a strong rear shear zone. (Left) Velocity vectors and strain rates across the model free surface. (Above) Velocity vectors and strain rates along cross section A-A´.

The rear shear zone is inactive in the model with a strong rear shear zone (ϕ_r = 7.5°). Strain is not partitioned across the bounding thrust fault and fault slip is oblique along its length.

Within the orogenic wedge, the horizontal convergence decreases to nearly zero. This results in material being uplifted vertically consistent with growth of the wedge via basal accretion. Thus, Model 1 behaves as a stable critical wedge orogen with no strain partitioning. The lack of strain partitioning in this case is predicted from the strength of the rear shear zone (i.e., Figure 2, point M1).

Model 2 - Weak rear shear zone (ϕ_r = 4°): Partial strain partitioning

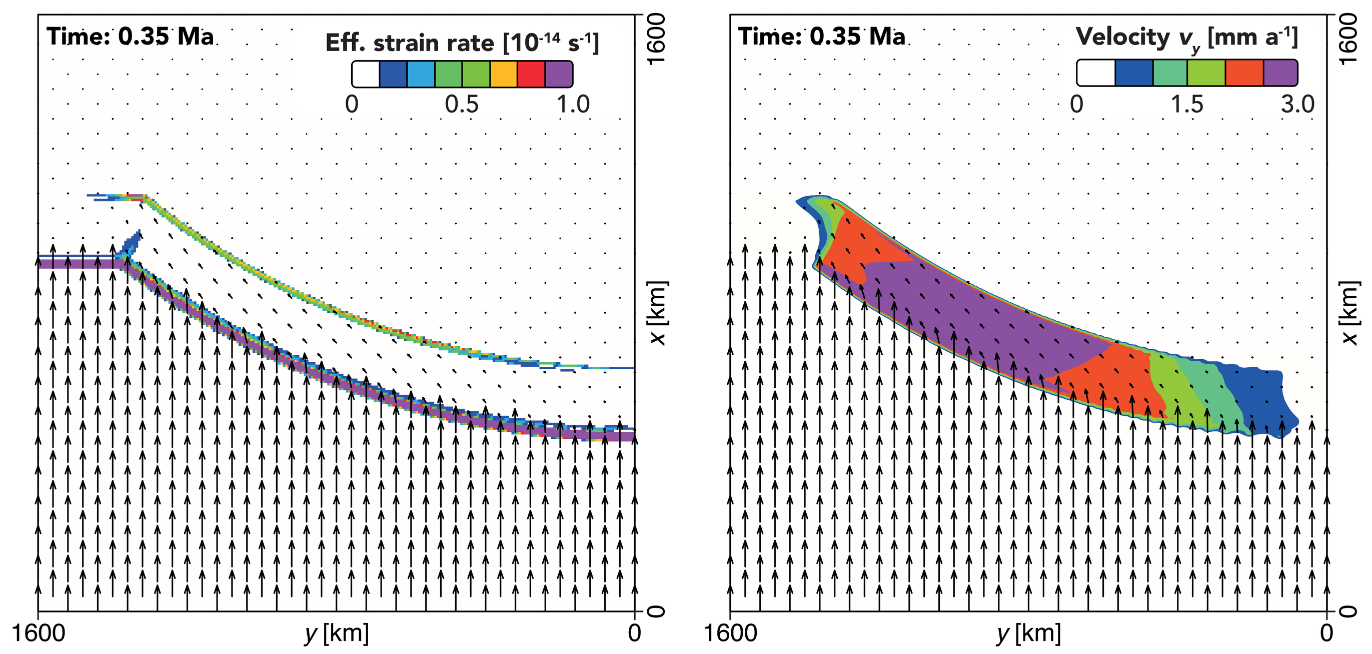

The reduction in strength of the rear shear zone to ϕ_r = 4° results in activation of that region as a strike-slip shear zone and strain partitioning develops in the parts of the orogen where the convergence obliquity angle exceeds ~10°. For sections of the orogen where the convergence obliquity is >20°, moderate strain partitioning is observed. Partitioning starts to develop for obliquity angles that are less than the theory requires (i.e., Figure 2, point M2), but the convergence velocity is not is not completely partitioned as would be required by the theory. Partitioning results in mass transport along strike at a rate of ~3 mm a^{-1}.

Figure 5. Experimental results for Model 2 with a weak rear shear zone. (Left) Velocity vectors and strain rates across the model free surface. (Right) Horizontal velocity component v_y and velocity vectors at the free surface.

Model 3 - Weak rear shear zone (ϕ_r = 4°), weak wedge (ϕ_w = 15→5°): Partial strain partitioning

Results for Model 3 are nearly identical to Model 2 and are presented below in Section 5.

5. General model behavior

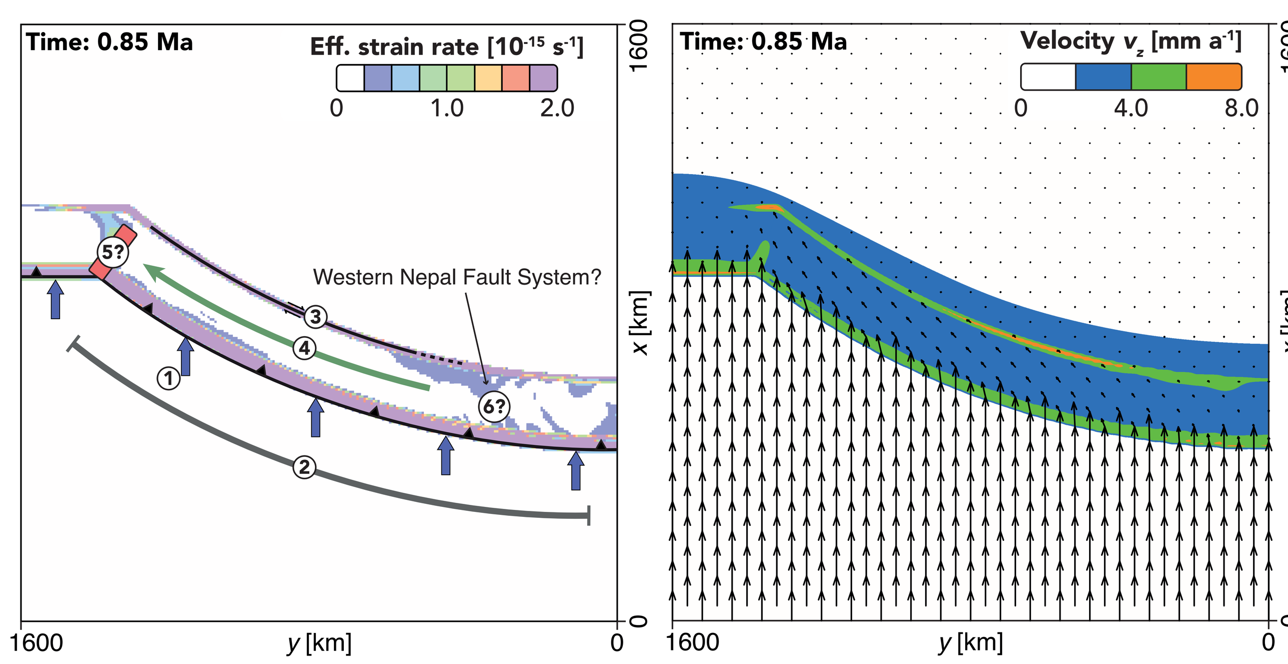

Figure 6. Model 3 results compared to the main aspects of an arcuate convergent orogen. (Left) Main aspects of an arcuate convergent orogen with strain rates. Feature labels as in Figure 1. (Right) Vertical velocity contours and velocity vectors for Model 3.

Models 2 and 3 nicely reproduce a number of the major features observed along the Himalayan arc (components 1-4). The rate of orogen-parallel mass transport owing to strain partitioning is relatively low compared to earlier results (Whipp et al., 2014), and likely leads to poor development of the extensional and shortening structures at the lateral ends of the partitioned region (components 5, 6). This results in reasonable uplift velocities in the orogenic wedge (2-4 mm a^{-1}), but uplift rates that are too low in the syntaxis (4-6 mm a^{-1}).

6. Conclusions

We make the following preliminary conclusions based on our 3D numerical experiments:

1. **Strain partitioning is predicted for an arcuate orogen of the scale of the Himalaya if the rear of the orogenic wedge is weak**
2. **Strain partitioning across the thrust front can produce an orogen-parallel velocity to supply additional mass into the Himalayan syntaxes**
3. **Although weakly expressed, the development of an extensional/strike-slip structure equivalent to the Western Nepal Fault System is observed in a location similar to its position in nature**

References

Braun, J., Thieulot, C., Fullsack, P., DeKool, M., Beaumont, C., and Huismans, R., 2008. DOUAR: A new three-dimensional creeping flow numerical model for the solution of geological problems. *Physics of the Earth and Planetary Interiors*, *171*(1), pp.76-91.
Murphy, M.A., Taylor, M.H., Gosse, J., Silver, C.R.P., Whipp, D.M., and Beaumont, C., 2014. Limit of strain partitioning in the Himalaya marked by large earthquakes in western Nepal. *Nature Geoscience*, *7*(1), pp.38-42.
Whipp, D.M., Beaumont, C., and Braun, J., 2014. Feeding the "aneurysm": Orogen-parallel mass transport into Nanga Parbat and the western Himalayan syntaxis. *Journal of Geophysical Research: Solid Earth*, *119*(6), pp.5077-5096.